

## Effect of the Annealing Gas and RF Power Sputtering in the Electrical, Structural and Optical Properties of ITO Thin Films

O. Boussoum<sup>1,\*</sup>, M.S. Belkaid<sup>1</sup>, C. Renard<sup>2</sup>, G. Halais<sup>2</sup>, F. Farhati<sup>1</sup>

<sup>1</sup> *Laboratory of Advanced Technologies of Genie Electrics (LATAGE), Department of Electronics, Faculty of Electrical and Computer Engineering, Mouloud Mammeri University (UMMTO), BP 17 RP 15000, Tizi-Ouzou, Algeria*

<sup>2</sup> *Centre de Nanosciences et Nanotechnologies, CNRS, Université Paris-Sud, 91405 Orsay Cedex, France*

(Received 18 December 2018; revised manuscript received 08 April 2019; published online 15 April 2019)

In the paper we propose to investigate the effect of the annealing gas and RF power sputtering on the electrical, structural and optical properties of indium tin oxide thin films for solar cells applications. These thin films were prepared on lightly doped silicon wafer by RF sputtering in Ar environment at room temperature and with a pressure of  $8 \cdot 10^{-3}$  mbar. Process parameters such as RF power and post deposition annealing were varied in order to determine their dependence on electrical, structural and optical properties of ITO thin films. Layer morphology and thickness measurements (with cross section) were investigated by scanning electron microscopy, and atomic force microscopy was performed to determine the surface roughness. The dependence of the resistivity, mobility and carrier concentration of these films by varying RF power and thermal annealing were studied by Hall Effect measurement. Spectroscopic ellipsometry was also used to determine the refractive index, thickness, roughness, porosity and optical bandgap of the films. Thus, the optical transmittance in the visible region was found to be above 85 %, the low resistivity and high mobility were found  $2.09 \cdot 10^{-4} \Omega \text{ cm}$  and  $35.81 \text{ cm}^2/(\text{V s})$ , respectively, for 200 nm thickness for the sample elaborated with a RF power of 150 W and an annealing at 400 °C for 10 min with rapid thermal annealing under  $\text{N}_2$ . The X-ray diffraction patterns of the thin films indicated a preferred orientation along the (222) plane, which provides a high degree of crystallinity for all  $\text{N}_2$  annealed samples. The XPS was used to determine oxidation states and identify the elemental content in the films. Obtained results for the surface morphology, electrical and optical properties of the ITO thin film details will be presented.

**Keywords:** Thin films, Indium tin oxide, Transparent conductor, Sheet resistance, RF Sputtering, Refractive index.

DOI: [10.21272/jnep.11\(2\).02010](https://doi.org/10.21272/jnep.11(2).02010)

PACS numbers: 73.61.Ph, 78.66.Bz

### 1. INTRODUCTION

Indium tin oxide (ITO) thin films are an n-type wide band-gap semiconductor. They are used in various applications due to the combination of three properties, namely, high transmittance in the visible and near IR regions (> 80 %), high band gap (3.2-4.3 eV) [1] and high carrier concentration ( $n \sim 10^{21} / \text{cm}^3$ ) generated by oxygen vacancy, as well as the substitution of  $\text{Sn}^{4+}$  for  $\text{In}^{3+}$  provide fairly low resistivity ( $< 10^{-3}$ ) [2]. The optimal Sn doping concentration is usually about 10 %.

ITO is widely used as a transparent electrode in a variety of optoelectronic devices, such as light-emitting diodes (LEDs) [3], top emitting VCSELs [4], liquid crystal displays (LCDs) [5], and as a transparent electrode for solar cell applications [6, 7]. Several deposition techniques are commonly used to prepare ITO thin films with high transmittance and low resistivity, such as chemical vapor deposition [8], spray pyrolysis [9], radio frequency plasma enhanced reactive thermal evaporation (rf-PERTE) [10], sol gel [11], activated reactive evaporation (ARE)[4], electron beam evaporation[1-2], DC and RF magnetron sputtering[10-12].

In this paper, we report on our studies of ITO thin films prepared with RF sputtering under various RF powers (60, 100 and 150 W) under Ar atmosphere at a pressure of  $8 \cdot 10^{-3}$  mbar, and no external heating of the substrate was performed. The effect of annealing gas (vacuum and  $\text{N}_2$  with a pressure of 5 and 1000 mbar,

respectively) was also investigated. The morphology, the electrical and optical properties of ITO thin films were studied.

### 2. MATERIALS AND METHOD

ITO thin films were prepared using RF sputtering at different RF power and an ITO target composed of  $\text{In}_2\text{O}_3:\text{SnO}_2$  (respectively, 90 % and 10 %) with a nominal purity of 99.99 %. The ITO thin films were deposited on lightly doped silicon and glass substrates at room temperature. The system was pumped up to  $10^{-6}$  mbar prior to deposition and removed from surface contamination of the target; it was pre-sputtered for 5 min. The film deposition process was carried out with Ar gas at a constant pressure (Fig. 1).

The silicon and glass substrates were first ultrasonically cleaned in acetone, ethanol and deionized water for 10 min and then dried under nitrogen gas. After this, silicon substrates were cleaned in  $\text{H}_2\text{SO}_4:\text{H}_2\text{O}_2:\text{H}_2\text{O}$  (3:1:1) for 5 min then rinsed for 3 min in deionized water with nitrogen bubbling. Finally, they were dipped in buffered HF (BHF) during 30 s, then rinsed for 3 min in deionized water with nitrogen bubbling.

In a first time, we have studied the deposition rate for different RF powers. Two types of post-deposition thermal treatments of the ITO thin films were carried out: the first one under vacuum at 5 mbar and the second one under  $\text{N}_2$  with a pressure of 1000 mbar and rapid thermal annealing for 10 min at 400 °C.

\* [boussoum.ouiza@gmail.com](mailto:boussoum.ouiza@gmail.com)

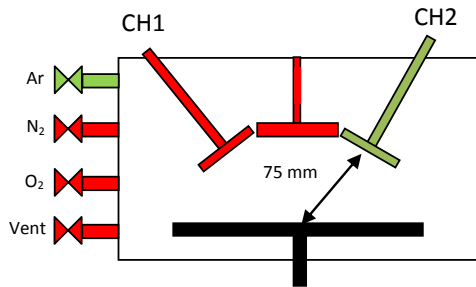


Fig. 1 – Schematic diagram of the sputtering system

For electrical characterization, the resistivity was estimated by the four-point method and hall-effect measurements, a scanning electron microscopy (SEM) was used to study the surface morphology. Spectroscopic ellipsometry was used to determine the optical properties. Atomic force microscopy (AFM) topographic images were collected in the tapping mode, the crystallographic orientation of ITO thin films was determined using X-Ray diffraction (XPRT PRO Philips). The surface chemical structure of ITO thin has been studied by X-ray photoelectron spectroscopy (XPS).

Table 1 – Deposition parameters

Deposition parameters	
RF Power sputtering	(150, 100, 60) W
Ar	36.6 sscm
Pressure	$8 \cdot 10^{-3}$ mbar
Sputtering time	(705, 1125, 1860) s
Substrate rotation	10 round/min
Target-substrate distance	75 mm
Temperature	Ambient

### 3. RESULTS AND DISCUSSION

#### 3.1 Electrical Properties

Fig. 2 shows the dependence of the resistivity, carrier concentration and mobility of the films as a function of RF power and annealing atmosphere. All films were deposited at a pressure of  $8 \cdot 10^{-3}$  mbar with Ar gas at room temperature. Samples annealed under N<sub>2</sub> atmosphere exhibited higher performances than those annealed under vacuum.

The resistivity decreases with an increase in the RF power for samples annealed under N<sub>2</sub> atmosphere and it increases for those annealed under vacuum. The lowest resistivity was found about  $2.1 \cdot 10^{-4} \Omega \text{ cm}$  for the sample deposited at RF power of 150 W and annealed under N<sub>2</sub>. The carrier concentration ( $n$ ) decreases from  $9 \cdot 10^{20} \text{ cm}^{-3}$  at RF power of 60 W to  $7 \cdot 10^{20} \text{ cm}^{-3}$  at 100 W, then it increases at RF power of 150 W for the annealing in N<sub>2</sub> atmosphere, whereas it decreases for the samples annealed under vacuum with an increase in RF power. High mobility was obtained for the sample deposited at RF power of 150 W and annealed in N<sub>2</sub> atmosphere.

#### 3.2 Optical Properties

The optical properties, specifically the complex refractive index  $N = n + ik$ , depend on the deposition parameters [12]. The optical constants,  $n$  and  $k$ , are referred to refractive index and extinction coefficient, respectively.

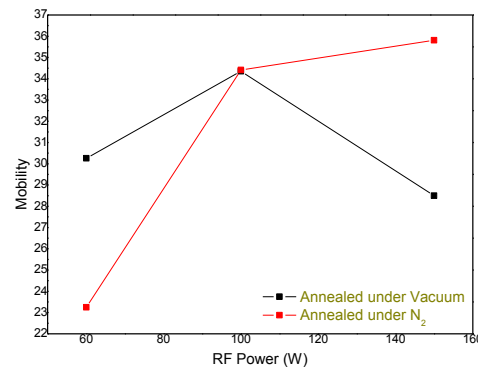
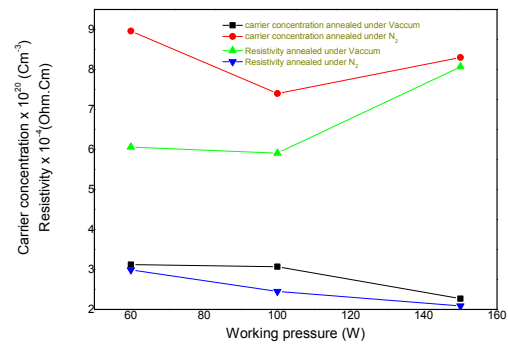


Fig. 2 – Variation of the resistivity, carrier concentration and mobility of ITO thin films grown at different RF power and annealed under various atmosphere (vacuum, N<sub>2</sub>)

To determine the optical constants, a variable angle spectroscopic ellipsometer (SE) in the spectral range 250-1700 nm (Woollam UV, V-Vase, IR region) was used.

The optical functions of ITO were described using a general oscillator model with an extended Drude model (EDM) used to correct classic Drude approximation for band-to-band transitions in the UV range, which is a combination of Lorentz-type oscillators [5].

#### Refractive index, porosity and optical band gap

Once the dielectric function is known, several material parameters of ITO can be determined such as refractive index, porosity and optical band gap. Values of the ITO thin film properties prepared at different RF powers and heated under vacuum and N<sub>2</sub> at a temperature of 400 °C for 10 min are detailed in Table 2.

In this study, the porosity values of the ITO films are determined from the following equation [13]:

$$Porosity = \left(1 - \frac{n^2 - 1}{n_d^2 - 1}\right) \times 100\%, \quad (1)$$

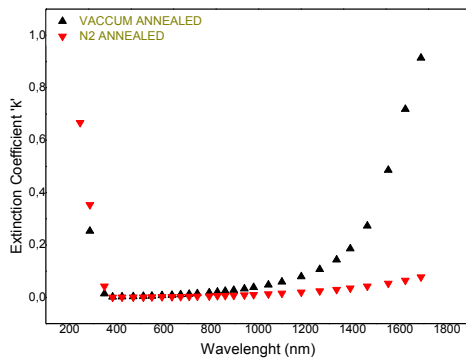
where  $n_d$  is the refractive index of pore-free ITO, which corresponds here to 2.1 [12], and  $n$  denotes the refractive index of the porous thin film. The porosity values calculated are listed in Table 2. It is seen that the porosity values decrease with the increase of RF power (N<sub>2</sub> or vacuum annealing), the maximum of porosity is about 21.21 % for the ITO thin films elaborated at 60 W and annealing in vacuum.

**Table 2** – Electro-optical characteristics of the ITO thin films elaborated with different RF powers and annealing atmospheres

Annealing atmosphere	In vacuum			In N <sub>2</sub>		
RF Power (W)	60	100	150	60	100	150
Refractive Index (n)	1.92	1.93	1.94	1.98	2.01	2.01
Porosity (%)	21.21	20.09	18.95	14.35	10.84	10.84

### The extinction coefficient $k$

We see in Fig. 3 that the extinction coefficient in the NIR range for samples annealed under vacuum is more important than those annealed in N<sub>2</sub> atmosphere, due to the free carrier absorption in this range. The optical constants displayed above show that all heat treatments improve the ITO transparency in the visible region and lower absorption in the NIR range.

**Fig. 3** – Extinction coefficient for samples elaborated with RF power of 60 W and annealing under vacuum and N<sub>2</sub> atmosphere at 400 °C

Optical band gap energy, refractive index, porosity, roughness of a semiconductor thin film are related to the transmittance (absorption) spectra [12]. For ITO thin film, in the visible and near IR spectra, the light incident on the film surface must be transmitted, reflected or absorbed.

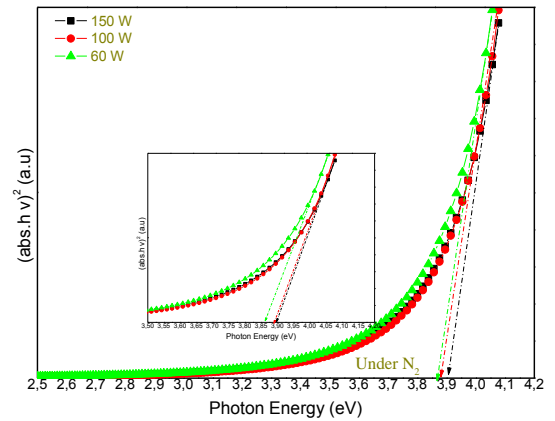
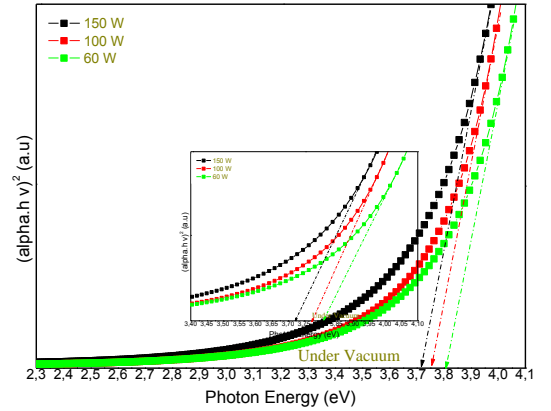
To determine the optical band gap energy of the films we used the expression of the optical absorption coefficient as a function of the light energy ( $h\nu$ ) by extrapolating the linear portion of the  $h\nu$  versus  $(ah\nu)^2$  curve to  $ah\nu = 0$ . The relationship between band gap and absorption coefficient is given by Tauc model [14]:

$$ah\nu \sim (h\nu - E_g)^{1/2}, \quad (2)$$

where  $a$  is the absorption coefficient, which is related to the extinction coefficient, by [15]:

$$\alpha = 4\pi k/\lambda \quad (3)$$

It can also be seen from Fig. 4 that the band gap increases with the increase of the RF power for the samples heated under N<sub>2</sub>, and it increases with the decrease of RF power for those annealed under vacuum. The ITO thin films annealed in N<sub>2</sub> present higher optical band (from 3.86 eV to 3.90 eV) than those annealed in vacuum (from 3.77 eV to 3.72 eV). It can be explained by the high carrier concentration of the films annealed in N<sub>2</sub> atmosphere.

**Fig. 4** – Variation of the optical band gap energy of 200 nm thick ITO layer deposited with different RF power annealed under vacuum and N<sub>2</sub> atmosphere

### Figure of merit

Performance of the transparent conductive materials is typically characterized by means of figure of merit that considers the electrical and optical properties of the thin films [16] defined by:

$$\Phi_{TC} = \frac{T^{10}}{R_s} = \left(\frac{t}{\rho}\right) e^{-10at}, \quad (4)$$

where  $T$  is the optical transmittance,  $t$  represents the thin film thickness,  $a$  is the absorption coefficient.

**Table 3** – Figure of merit dependence of RF power and annealing atmosphere at 550 nm

RF Power	In vacuum	In N <sub>2</sub>
60 W	0.1724	0.2951
100 W	0.1772	0.3803
150 W	0.1134	0.4282

Table 3 reports the dependence of  $\Phi_{TC}$  in RF power and annealing atmosphere. The fundamental characteristics of the transparent conductors are absorption  $\alpha$  (transmittance) and resistivity  $\rho$ , for which  $\Phi_{TC}$  has to present a maximum value [17].

The samples elaborated at RF power of 150 W and annealed in  $N_2$  atmosphere present high figure of merit with low resistivity and low absorption (high transmittance).

### 3.3 Morphology Properties

#### Scanning electron microscope (SEM)

A scanning electron microscope (Hitachi SU 8000) was used to study the surface morphology and measure the thickness of the ITO thin films. The substrates were rotated at 10 tr/min during the deposition to ensure even coatings. Deposition rate ( $r$ ) was inferred from the thickness of the thin film removed from the deposition chamber, and corresponds to deposition time. The deposition rate was found 6.42 nm/min, 10.66 nm/min and 17.00 nm/min for the samples elaborated under RF power of 60 W, 100 W and 150 W, respectively.

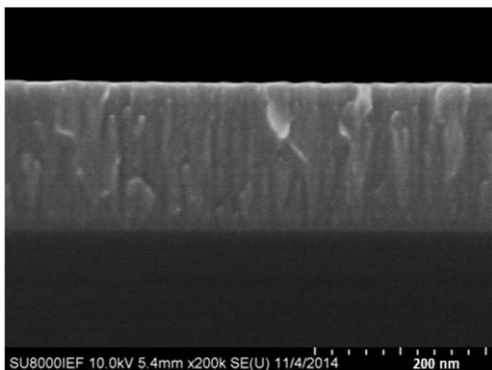
The deposition rate increases with increasing RF power. These changes in the deposition rate from the RF power can be explained as follows: at high RF power, argon ions have more energy to pull atoms and molecules out the target; therefore the amount of materials deposited in the substrate become bigger.

Fig. 5a shows the SEM images from the cross section of ITO film deposited on silicon substrate at room temperature. It is seen that the ITO film grown by RF sputtering has a fine columnar structure.

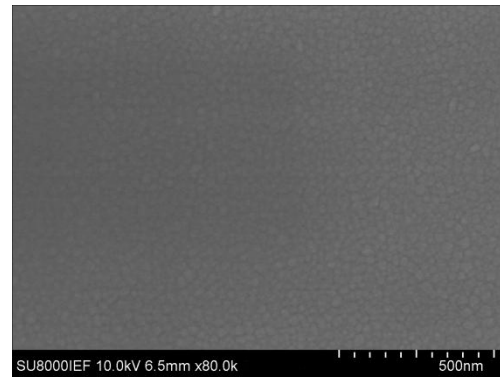
Evolution of surface microstructure dependence on the heat treatment at different gas was observed by SEM. The samples elaborated at RF power of 150 W are illustrated in Fig. 5b, annealed under  $N_2$ , (c) annealed under vacuum. We see that the films are rather uniform and have granular structure. Sample annealed under vacuum present crack that is what proves the high resistivity of the film. The same morphology was observed for other RF power.

#### Atomic force microscopy (AFM)

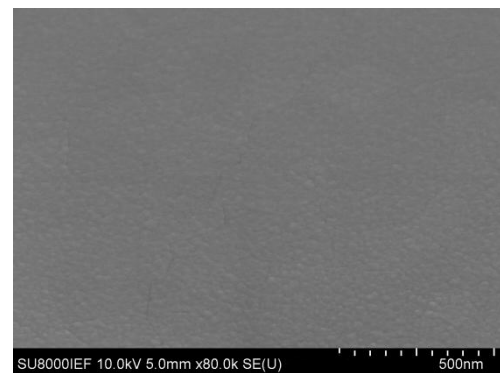
Atomic force microscopy (AFM) in tapping mode was used to probe the surface morphology obtained by SEM results; AFM images of the ITO thin films reveal the formation of a porous granular surface. Other ITO samples show similar morphology.



a



b



c

**Fig. 5** – (a) SEM images from the cross section of the ITO film deposited on Si at room temperature, (b) SEM images of the surface of ITO annealed under  $N_2$ , (c) annealed under vacuum

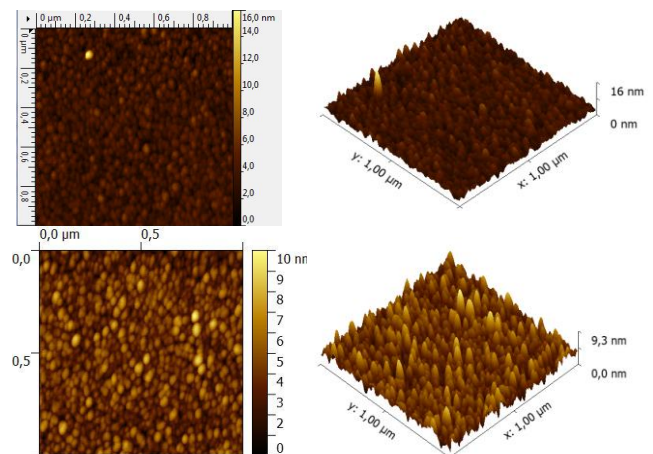


**Fig. 6** – 2D and 3D AFM pictures of the surface roughness of the ITO thin film annealed under  $N_2$  atmosphere and in vacuum, respectively

The 2D and 3D surface morphology, the root-mean-square (RMS) surface and average roughness ( $R_a$ ) of ITO thin films annealed under different atmosphere are observed by AFM. The results are shown in Fig. 6. The ITO deposited at RF power of 60 W and annealed under  $N_2$  atmosphere show a surface roughness of only 1.08 nm and those annealed under vacuum show RMS of 1.19 nm. At high RF power (150 W), the surface roughness was found 2.50 nm and 1.37 nm for the samples annealed under vacuum and  $N_2$ , respectively.

### X-ray diffraction (XRD)

To investigate the structure dependence on the RF power deposition and annealing atmosphere, the X-ray diffraction analysis was performed between  $20^\circ$  and  $90^\circ$  for the ITO thin films using a XPERT PRO X-ray Diffractometer in parallel beam geometry with Cu-K $\alpha$  radiation (Ratio K-Alpha2/K-Alpha1 = 0.5000) at 45 kV and 40 mA. The ITO thin films annealed under vacuum and deposited at RF power (60 W, 100 W) revealed an amorphous structure, at high RF power (150 W) polycrystalline structure was developed with cubic bixbyite phase In $_2$ O $_3$  ((222) plane). The XRD peaks corresponding to the (211), (400), (440), (622) planes appeared clearly. All samples annealed under N $_2$  atmosphere exhibit a polycrystalline cubic bixbyite phase In $_2$ O $_3$  structure with more intensity of diffraction with increasing RF power. At RF power of 100 W and 150 W other peaks are identified from (411) (422), (135) planes.

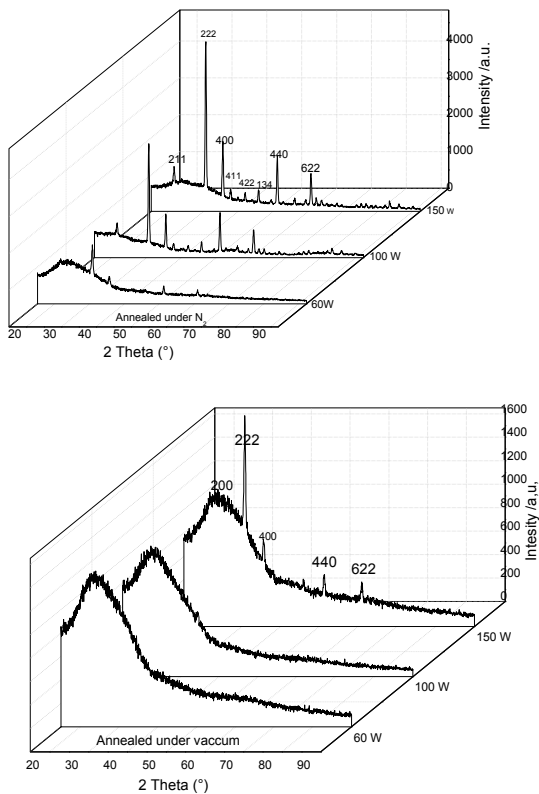


**Fig. 7** – X-ray diffraction patterns of ITO thin films elaborated at different RF power and annealed under different atmospheres

The ratio between the peak intensities of (222) and (400) planes assumes the crystal quality parameter. The I $_{222}$ /I $_{400}$  values are 6.96 and 4.23 for the samples elaborated at RF power of 150 W and annealed under N $_2$  atmosphere and under vacuum, respectively, this ratio was found higher than 3.3 standard value of the crystalline ITO powder [9]. The highest intensity of (222) peak is obtained for the samples heated under N $_2$  atmosphere confirming better crystallinity.

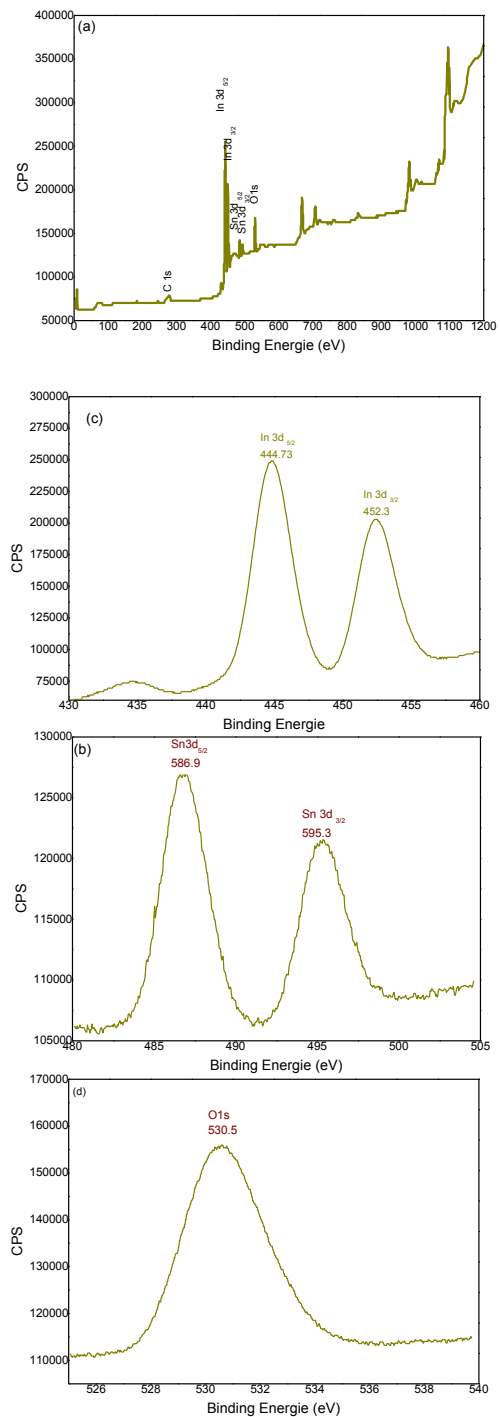


**Fig. 8** – XPS spectra: (a) wide scan spectra, (b) Sn 3d, (c) In 3d, and (d) O 1s peaks for the ITO film deposited at RF power of 150 W and annealed under N $_2$  atmosphere

### X-ray photoelectron spectroscopy

We show the X-ray photoelectron spectroscopy (XPS) spectra for ITO elaborated at RF power of 150 W and annealed under N $_2$  atmosphere, which represent the photoelectron peaks for In, Sn and O. In the spectra, the

binding energy was defined from 0 to 1200 eV. A binding energy of 1s peak of carbon (C) appears at 284 eV, the presence of the peaks is related to surface contamination, which corresponds to the fact that the samples were kept in plastic boxes and were exposed to air.

The XPS spectra for the Sn 3d, In 3d doublets and O 1s are reported in Fig. 8b, c, d, respectively, for the ITO thin film elaborated under RF power of 150 W and annealed under N<sub>2</sub> atmosphere.

Fig. 8b shows the XPS spectra of Sn 3d, the peaks located at 486.9 and 495.3 eV were assigned to Sn 3d<sub>5/2</sub> and Sn 3d<sub>3/2</sub>, respectively, this binding corresponds to the Sn<sup>+4</sup> bonding state in the ITO [9-23]. As seen from Fig. 8c, the In 3d<sub>3/2</sub> and In 3d<sub>5/2</sub> peaks are observed at 444.73; 452.3 eV expresses the In<sup>+3</sup> bonding state from In<sub>2</sub>O<sub>3</sub> [19].

The binding energy of the O 1s peak is observed at 530.5 eV, peaks of oxygen are bonded both with indium and tin [20]. According to the XPS analysis, this peak is assigned to oxygen vacancies, the obtained results are in good agreement with typical crystalline ITO reported in previous studies [9, 21, 22].

**Table 4** – Position of O 1s, In 3d and Sn 3d peaks dependence on RF power and annealed under N<sub>2</sub> atmosphere

RF power	O 1s	In 3d	Sn 3d
60 W	530.37	444.76	486.88
100 W	530.37	444.76	486.6
150 W	530.5	444.73	486.9
ITO-Crist. [20]	530.1	444.6	486.4
ITO-amorphous [20]	531.4	445.0	–
ITO-RTA-Crist. annealed [22]	–	444.3	486.3

## REFERENCES

1. D. Raoufi, F. Hosseinpanahi, *J. Mod. Phys.* **3** No 8, 645 (2012).
2. D. Choi, S.-J. Hong, Y. Son, *Materials* **7** No 12, 7662 (2014).
3. K.D. Vanyukhin, R.V. Zakharchenko, N.I. Kargin, L.A. Seidman, *Russ. Microelectron.* **43** No 8, 569 (2014).
4. T. Camps, V. Bardinal, E. Havard, M. Condé, C. Fontaine, G. Almuneau, L. Salvagnac, S. Pinaud, J.B. Doucet, *Eur. Phys. J. D* **59** No 1, 53 (2010).
5. M. Duta, M. Anastasescu, J.M. Calderon-Moreno, L. Predoana, S. Preda, M. Nicolescu, H. Stroescu, V. Bratan, I. Dascalu, E. Aperathitis, M. Modreanu, M. Zaharescu, M. Gartner, *J. Mater. Sci. Mater. Electron.* **27** No 5, 4913 (2016).
6. X. Yan, F.W. Mont, D.J. Poxson, M.F. Schubert, J.K. Kim, J. Cho, E.F. Schubert, *Jpn. J. Appl. Phys.* **48** No 12, 120203 (2009).
7. R.N. Chauhan, C. Singh, R.S. Anand, J. Kumar, *Int. J. Photoenergy*, **2012**, 1 (2012).
8. G.G. Pethuraja, R.E. Welsler, A.K. Sood, C. Lee, N.J. Alexander, H. Efstathiadis, P. Haldar, J.L. Harvey, *Adv. Mater. Phys. Chem.* **2** No 2, 59 (2012).

Table 4 shows dependence of O 1s, In 3d and Sn 3d on RF power for the samples annealed under N<sub>2</sub> atmosphere. According to XPS analysis, the binding energy of the peaks O 1s, In 3d and Sn 3d are in good agreement with typical crystalline ITO reported in pervious works.

## 4. CONCLUSIONS

In this work, we have analyzed the influence of the RF power and annealing gas on the electrical, optical and structural characteristics of indium tin oxide (ITO) films deposited on low-doped silicon and glass substrate at room temperature. Atomic force microscopy (AFM), SEM and ellipsometry, X-Ray diffraction (XRD), X-ray photoelectron spectroscopy (XPS) were used to characterize the films, and Hall effect was used to determine the electrical properties.

Samples annealed under N<sub>2</sub> atmosphere exhibit better characteristics than those annealed under vacuum.

All the films annealed under N<sub>2</sub> atmosphere confirmed a better crystallinity with (222) preferred orientation. The intensity of the peak (222) increases with the increase of RF power. The best optoelectronic performance was obtained at RF power of 150 W, it shows a high optical band gap of about 3.90 eV (high transmittance), a low specific resistivity  $2.09 \cdot 10^{-4} \Omega \cdot \text{cm}$  (high figure of merit), and a carrier mobility of  $35.81 \text{ Cm}^2\text{V}^{-1}\text{s}^{-1}$ . These ITO thin films are suitable for optoelectronics applications.

## ACKNOWLEDGEMENTS

This work was done with the CTU IEF-MINERVE facility and partly supported by the RENATECH network and the General Council of Essonne, France.

9. S. Marikkannu, C. Sanjeeviraja, S. Piraman, A. Ayeshamariam, *J. Mater. Sci. Mater. Electron.* **26** No 4, 2531 (2015).
10. C. Nunes de Carvalho, G. Lavareda, E. Fortunato, P. Vilarinho, A. Amaral, *Mater. Sci. Eng. B* **109** No 1-3, 245 (2004).
11. H. Cho, Y.-H. Yun, *Ceram. Int.* **37** No 2, 615 (2011).
12. V. Dimitrov, S. Sakka, *J. Appl. Phys.* **79** No 3, 1741 (1996).
13. J.-W. Ok, D.-J. Kwak, S.-H. Kim, Y.-M. Sung, *Vacuum*, **110**, 196 (2014).
14. G. Yildirim, M. Akdogan, A. Varilci, C. Terzioğlu, *Cryst. Res. Technol.* **45** No 11, 1161 (2010).
15. G. Haacke, *J. Appl. Phys.* **47** No 9, 4086 (1976).
16. L. Álvarez-Fraga, F. Jiménez-Villacorta, J. Sánchez Marcos, A. de Andrés, C. Prieto, *Appl. Surf. Sci.* **344**, 217 (2015).
17. Y.J. Kim, S.B. Jin, S.I. Kim, Y.S. Choi, I.S. Choi, J.G. Han, *J. Phys. Appl. Phys.* **42** No 7, 75412 (2009).
18. M. Chuang, *J. Mater. Sci. Technol.* **26** No 7, 577 (2010).
19. <http://www.jmst.org/EN/Y2010/V26/I7/577>
20. D. Spyros, arXiv: cond-mat.mtrl-sci/ 1210.0035v1.
21. H. Lee, S.W. Cho, *Appl. Sci. Conver. Technol.* **25** No 6, 128 (2016).
22. J.B. Plumley, A.W. Cook, C.A. Larsen, K. Artyushkova, S.M. Han, T.L. Peng, R.A. Kemp, *J. Mater. Sci.* **53** No 18, 12949 (2018).

**Вплив нагрівання газу і RF потужності розпилення на електричні, структурні та оптичні властивості тонких плівок ІТО**O. Boussoum<sup>1</sup>, M.S. Belkaid<sup>1</sup>, C. Renard<sup>2</sup>, G. Halais<sup>2</sup>, F. Farhati<sup>1</sup>

<sup>1</sup> *Laboratory of Advanced Technologies of Genie Electrics (LATAGE), Department of Electronics, Faculty of Electrical and Computer Engineering, Mouloud Mammeri University (UMMTO), BP 17 RP 15000, Tizi-Ouzou, Algeria*

<sup>2</sup> *Centre de Nanosciences et Nanotechnologies, CNRS, Université Paris-Sud, 91405 Orsay Cedex, France*

У роботі пропонується дослідити вплив нагрівання газу та RF потужності розпилення на електричні, структурні та оптичні властивості тонких плівок оксиду індію для застосувань у сонячних елементах. Ці тонкі плівки готували на слаболегованій кремнієвій пластині методом RF-розпилення у середовищі Ar при кімнатній температурі і тиску  $8 \cdot 10^{-3}$  мбар. Параметри процесу, такі як RF потужність і відпал після осадження, змінювалися для того, щоб визначити їх залежність від електричних, структурних і оптичних властивостей тонких плівок ІТО. Морфологію та вимірювання товщини шару (з поперечним перерізом) досліджували методом скануючої електронної мікроскопії, а для визначення шорсткості поверхні застосовували атомну силову мікроскопію. Залежність питомого опору, рухливості та концентрації носіїв цих плівок досліджували за допомогою ефекту Холла шляхом зміни RF потужності та термічного відпалу. Спектроскопічна еліпсометрія також використовувалася для визначення показника заломлення, товщини, шорсткості, пористості та оптичної ширини забороненої зони плівок. Таким чином, оптичний коефіцієнт пропускання у видимій області виявився вище 85 %; низький питомий опір і висока рухливість становили, відповідно,  $2.09 \cdot 10^{-4}$  Ом·см і  $35.81$  см<sup>2</sup>/(V·с) для товщини зразка 200 нм, RF потужності 150 Вт, і відпалу при 400 °C протягом 10 хв при швидкому термічному відпалі під дією N<sub>2</sub>. Рентгенівська дифракція тонких плівок показала кращу орієнтацію вздовж напрямку (222), яка забезпечує високу ступінь кристалічності для всіх відпалених N<sub>2</sub> зразків. Рентгенівська фотоелектронна спектроскопія використовувалася для визначення станів окислення та елементного вмісту у плівках. Представлені результати морфології поверхні, електричні та оптичні властивості плівки ІТО.

**Ключові слова:** Тонкі плівки, Оксид олова та індію, Прозорий провідник, Опір листа, RF розпилення, Показник заломлення.